AJNR

CNS Vasculitis in Autoimmune Disease: MR Imaging Findings and Correlation with Angiography

Martin G. Pomper, Timothy J. Miller, John H. Stone, William C. Tidmore and David B. Hellmann

AJNR Am J Neuroradiol 1999, 20 (1) 75-85
http://www.ajnr.org/content/20/1/75

AJNR Am J Neuroradiol 20:75–85, January 1999

CNS Vasculitis in Autoimmune Disease: MR Imaging Findings and Correlation with Angiography

Martin G. Pomper, Timothy J. Miller, John H. Stone, William C. Tidmore, and David B. Hellmann

BACKGROUND AND PURPOSE: **MR findings in CNS vasculitis and their correlation with angiography have not been clearly defined. We therefore explored three hypotheses regarding CNS vasculitis associated with autoimmune disease: 1) MR imaging is highly sensitive; 2) a typical MR appearance exists; and, 3) MR and angiographic findings correlate well.**

METHODS: **We studied 18 patients with CNS vasculitis associated with autoimmune disease, characterized the MR lesions by type, size, number, and location, and correlated the MR findings with those of angiography.**

RESULTS: **All patients with CNS vasculitis had abnormalities on MR studies. On average, four ± two lesions per patient were detected on MR images. The lesions were located in the subcortical white matter (n = 20), cortical gray matter (n = 16), deep gray matter (n = 16), deep white matter (n = 9), and cerebellum (n = 9). Only 65% of MR lesions were evident on angiograms; 44% of the lesions revealed on angiograms were detected by MR.**

CONCLUSION: **MR imaging is sensitive for CNS vasculitis. Lesions attributable to CNS vasculitis in autoimmune disease are distributed nearly equally among cortical, subcortical, and deep gray matter structures. The modest correlation between MR imaging and angiography suggests that the two techniques provide different information about CNS vasculitis and that both types of studies are needed for the complete assessment of damage caused by vascular abnormalities.**

CNS vasculitis represents a heterogeneous group of inflammatory diseases that primarily affect the small leptomeningeal and parenchymal blood vessels of the brain (1). A variety of neurologic insults may cause CNS vasculitis, including infection, malignancy, ionizing radiation, cocaine ingestion, and autoimmune disease (1, 2). Primary angiitis of the CNS (2–4), systemic lupus erythematosus (5), polyarteritis nodosa (6), giant cell arteritis (1), and Sjögren syndrome (7) comprise the majority of autoimmune conditions associated with CNS vasculitis. In all these disorders, the precise pathogenesis remains obscure; in all, however, the immune system appears to play a central role, and immunosuppressive agents are the cornerstones of treatment. In practice, MR imaging precedes angiographic studies in the evaluation of patients. Because of the limited data available on the use of MR imaging in CNS vasculitis (4, 8–12), we reviewed our experience with this disorder. We hypothesized that MR imaging is highly sensitive, that a typical MR appearance exists, and that MR and angiographic findings correlate well.

Received June 25, 1997; accepted after revision August 26, 1998.

From the Departments of Radiology (M.G.P.) and Medicine (J.H.S., W.C.T., D.B.H.), The Johns Hopkins University School of Medicine, The Johns Hopkins Hospital, Baltimore; and the Department of Radiology (T.J.M.), Good Samaritan Hospital, Cincinnati.

Address reprint requests to David B. Hellmann, MD, The Johns Hopkins Hospital, 1830 E Monument St, Room 9030, Baltimore, MD 21205.

Methods

The entry criteria for the study included all of the following: 1) an angiogram interpreted as positive (see definition below) for CNS vasculitis by the attending neuroradiologist at the time the angiogram was obtained; 2) a clinical history consistent with CNS vasculitis, that is, clinical findings of an acquired neurologic deficit that remained unexplained after a thorough initial evaluation (9); and 3) exclusion of nonautoimmune causes of the patient's presentation (eg, infection, malignancy, ionizing radiation, and cocaine use). Of 259 angiograms obtained at our hospital to exclude CNS vasculitis between 1986 and 1997, 30 revealed abnormalities. Of those 30 patients, 20 had autoimmune disorders. Of those 20 patients, 16 had angiograms and MR studies available for review; these 16 patients, along with two patients referred from outside institutions, were included in the study (total patients = 18).

Three rheumatologists and one medical resident reviewed the patients' medical records using a defined protocol and a data abstraction form. The information collected during the medical records review included the following: age, gender, and history of previous rheumatic diseases; risk factors for atherosclerotic vascular disease; neurologic symptoms and deficits at presentation; lumbar puncture results; original interpre-

TABLE 1: Population characteristics

Patient	Age (y)/Sex	Diagnosis
1	60/F	PACNS
2	37/F	SLE
3	33/F	PACNS
4	71/F	PACNS
5	41/F	PACNS
6	24/F	PACNS
7	59/M	PACNS
8	14/F	PACNS
9	50/F	PACNS
10	50/F	PACNS
11	19/M	PACNS
12	74/M	PACNS
13	53/F	PACNS
14	52/F	PACNS
15	51/M	PACNS
16	31/F	SLE
17	40/F	PAN
18	55/M	GCA

Note.—PACNS indicates primary angiitis of the CNS; SLE, systemic lupus erythematosus; PAN, polyarteritis nodosa; GCA, giant cell arteritis.

tations of all MR studies and angiograms; and the results of brain biopsies and postmortem studies. Brief clinical summaries were written for each patient. The presence or absence of oligoclonal bands in patients' CSF and serum antiphospholipid antibodies were also noted, but not included, in the analysis because of the small number of patients who had such tests. Patients with a history of diabetes and hypertension were excluded. No patient had multiple sclerosis or other demyelinating diseases.

MR imaging was performed on a 1.5-T imaging system. Spin-echo (SE) T1-weighted sagittal (600/20 [TR/TE]) and double-echo (T2-weighted) axial (3000/30,100) images were obtained for all patients. In one patient (patient 6), a fluid-attenuated inversion recovery (FLAIR) sequence (11004/114; TI = 2200) was also obtained. Intravenous gadopentetate dimeglumine (0.2 mL/kg) was administered to 11 patients (patients 1, 2, 4, 6–9, and 11–14), and contrast-enhanced T1-weighted images were subsequently obtained in the axial and/or coronal planes (600/20–30). MR angiography was performed in six patients (patients 4, 6, 9, 10, 13, and 14), using 3D time-of-flight imaging. Conventional biplane film screen or digital subtraction angiography was performed in all patients. Details of the angiographic procedures have been described previously (12).

Angiographic and MR findings were considered positive if interpreted by the attending neuroradiologist as being consistent with vasculitis. To evaluate the consistency of the radiologic diagnoses and to perform correlations between MR imaging and angiography, all the available radiologic studies were reviewed by two additional attending neuroradiologists who were blinded to both the clinical data and the results of other radiologic studies. Discrepancies between the reviewers were submitted to a third attending neuroradiologist for arbitration. The reviewers considered an angiogram to have positive findings if focal or diffuse areas of arterial stenosis, occlusion, dilatation, or beading were detected (1, 9); MR findings were considered positive if foci of high signal intensity were present on long-TR images. To reduce the likelihood of including in our analysis T2 bright lesions caused by small-vessel atherosclerotic disease, we excluded patients with a history of hypertension or diabetes.

We determined the type, size, and number of all lesions detected by MR imaging, and assigned each lesion to a vascular distribution using a standard atlas (13). We classified the lesions as occurring in the following brain regions: cortical gray matter, subcortical white matter, deep white matter, deep gray matter, and cerebellum. We distinguished subcortical white matter from deep white matter by defining the former as the region directly adjacent to the cortex and the latter as a region clearly separate from the cortex; for example, a periventricular or internal capsule location. To be classified as periventricular, a lesion had to be focal and adjacent to the ventricle. The volume of a lesion was estimated by tracing the lesion manually and then calculating the product of the dimensions. The reported volume for each lesion was the average of the two reviewers' estimates. When the reviewers' estimates varied more than twofold, one of the reviewers quantified the volume of the lesion in question using MedVol 1.7 (software; copyright by Bruce E. Hall, MD, The Johns Hopkins University, Baltimore, MD) and reported that measurement. We correlated the lesions detected on MR images with those found on angiograms for all patients for whom both MR images and complete (at least three-vessel) angiograms were obtained (patients 9 and 14 were excluded from the correlation studies because of incomplete angiograms). If an MR lesion fell within a vascular territory in which a clear lesion existed on the corresponding angiogram, the two lesions were judged to correlate.

We used the Scheffé test to compare the frequency of lesion occurrence in MR vascular distributions. Differences were considered significant if P values were less than .05. Statistical analysis was performed using StatView SE + Graphics 1.03 (Abacus Concepts Inc, 1988).

Results

For each patient, the demographic characteristics and diagnoses associated with CNS vasculitis are displayed in Table 1. Thirteen of the 18 patients were female (72%) and five were male (28%). The patients ranged in age from 14 to 74 years, with a mean age of 45 ± 14 years. No patient had a history of hypertension, and none had used cocaine within 3 years of disease onset.

MR Imaging

Abnormalities were revealed on the MR studies in all patients with angiographically proved CNS vasculitis. Among the 18 patients, a total of 74 vascular, parenchymal, and extraaxial lesions (each representing one row in Table 2) were detected by MR imaging, an average of four ± two lesions per patient. The number of lesions per patient ranged from as few as one to as many as nine (Figs 1 and 2). Fourteen (78%) of the 18 studies revealed bilateral disease, and 13 (72%) detected exclusively supratentorial lesions. No patient had infratentorial lesions in the absence of supratentorial findings. Some lesions extended over more than one brain region. Among the 74 lesions, 20 were located in the subcortical white matter, 16 in the deep gray matter, 16 in the cortical gray matter, nine in the deep white matter, and nine in the cerebellum. Three carotid occlusions and one subarachnoid hemorrhage (SAH) were also detected. Regarding the territories affected, the middle cerebral artery (MCA) (average, 2.3 lesions per patient) was more frequently affected than the anterior cerebral artery (ACA) (average, 0.2 lesions per patient), the pos-

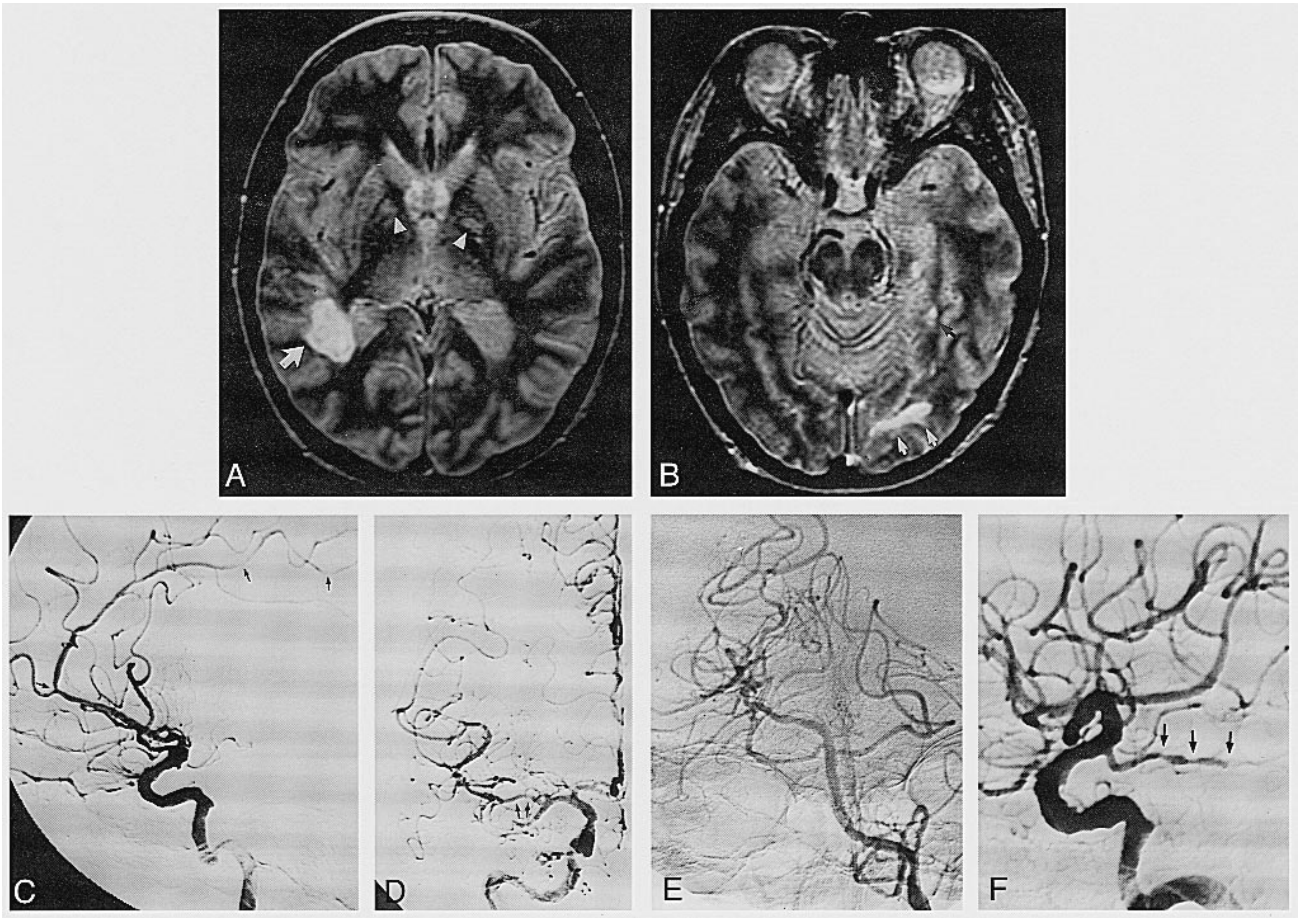

FIG 1. Patient 1: 60-year-old woman with primary angiitis of the CNS (a typical case of CNS vasculitis).

A and *B*, Axial SE MR images (3000/34). In *A*, an infarct is seen in the right subcortical white matter and the deep white matter (posterior MCA distribution) (*arrow*). Lacunar infarcts are also present in the globus pallidi (*arrowheads*). In *B*, infarcts are present in the left subcortical white matter (PCA distribution) (*white arrows*) and posterior left hippocampus (*black arrow*). Increased signal in the putamina and midbrain are artifactual.

C, Right lateral digital subtraction angiogram reveals mild narrowing of the proximal (near the A2 segment bifurcation) and several distal pericallosal artery segments (*arrows*). The MCA is poorly visible.

D, Anteroposterior digital subtraction angiogram of the right common carotid artery shows significant narrowing of the right M2 segment (*arrows*), with consequent attenuation of the more distal segments. The left MCA was normal.

E and *F*, Anteroposterior left vertebral artery (*E*) and lateral left common carotid artery (*F*) injections depict a fetal origin of the left PCA, with beading and occlusion of the PCA (*arrows* in *F*) and correlate with the MR image shown in *B*.

terior cerebral artery (PCA) (average, 0.7 lesions per patient), or the vertebral artery (average, 0.5 lesions per patient) territories ($P < .05$).

The lesions included 17 classic wedge-shaped infarctions in the cortical gray matter or cortical gray matter plus subcortical white matter (Fig 2A and B). The volume of the infarctions ranged from 0.1 to 80 cm^3, with a mean of 11.4 cm^3 (median, 2.2 cm^3). Two patients (patients 3 and 12) had parenchymal lesions associated with hemorrhage (Fig 3). Only three strictly periventricular lesions (in three different patients) were identified (Fig 4B and D). The lesion in Figure 1A was considered to reside in the subcortical white matter, because more superior images (not shown) placed the majority of this lesion in that region rather than in a periventricular location.

Correlation of MR Imaging with Angiography

Lesions involving 74 arteries were revealed by angiography. The angiographic results are presented in Table 3. A median of 6.5 days elapsed between MR imaging and angiography. We correlated the MR results with the angiographic findings on a lesion-for-lesion basis. The correlation between MR imaging and angiography is summarized in Table 4. Angiography detected 43 (65%) of the 66 lesions evident on MR images. In comparison, MR imaging detected 30 (44%) of the 68 angiographic lesions.

CNS pathologic specimens were available in four patients, one from autopsy (patient 15) and three from brain biopsies (patients 1, 2, and 4). In patients 2, 4, and 15, the clinical diagnosis of CNS vasculitis was confirmed by pathologic findings. In patient 1, the brain biopsy samples revealed no abnormalities.

Discussion

CNS vasculitis occurs frequently in the differential diagnosis of patients with neurologic signs

TABLE 2: Lesions on MR images

Patient	Location of Lesion	Lesion Size (cm^{13})	Vascular Distribution	No. of Affected Brain Regions	Time (y)
1	R CGM	15	MCA	4	1
	R SCWM	2	MCA		
	R SCWM	0.2	MCA		
	R DWM	0.2	MCA		
	R CB	0.1	SCA		
	L SCWM	1	PCA		
2	R CGM, SCWM	50	MCA	6	7
	R CGM, SCWM	50	PCA		
	R DGM	8	MCA		
	L CGM, SCWM	50	PCA		
	L DGM	3	MCA		
	L SGWM	6	MCA		
3	R CGM, DGM, SCWM	60	MCA	8	5
	R cavernous, carotid (occluded)				
	L CGM, DGM, SCWM	40	MCA		
	L cavernous, carotid (occluded)				
4	R DGM	0.4	MCA	3	11 mo
	R DGM	0.1	MCA		
	R DGM	0.1	PCA		
	R SCWM	0.3	MCA		
	L DGM	0.1	MCA		
	L DGM	0.6	MCA		
5	L parietal subarchanoid space	…	…	1	9
6	L CGM, DGM, SCWM	35	MCA	3	27
7	R CGM	15	MCA	5	10
	R DGM, DWM	15	MCA		
	R CB	0.3	AICA		
	L DGM	0.2	MCA		
8	R CGM	12	PCA	2	6
	R CGM	2.5	MCA		
	L CGM	12	PCA		
	L CGM	2	MCA		
9	R CGM, SCWM	70	MCA	5	2.5 mo
	L CGM, SCWM	80	PCA		
	L CGM, SCWM	7	MCA		
	L CB	7	PICA		
10	R DWM	0.6	PCA	3	1
	L SCWM	0.5	MCA		
	L DWM	0.6	MCA		
11	R CGM	6	PCA	4	7
	R DGM, DWM	2.5	MCA		
	R DWM	7	MCA		
	L DWM	1	BA		
12	R CGM, SCWM	10	PCA	2	1
	R SCWM	0.7	MCA		
13	R DGM	0.5	MCA	6	5
	R DGM	0.1	MCA		
	R SCWM	1.3	ACA		
	R DWM	1.4	MCA		
	R CB	8	PICA		
	R CB	8	PICA		
	L DGM	0.2	PCA		
	L DGM	0.1	MCA		
	L CB	3	PICA		
14	R DGM	1	MCA	5	3
	L CGM, SCWM	50	ACA		
	L DGM	3	MCA		
	L DWM	3	MCA		
15	R CGM, DGM, SCWM	50	MCA	4	13
	R supraclinoid carotid (occluded)				
16	R SCWM, DWM	10	MCA	4	7
	L CGM	12	ACA		
	L DWM	1	MCA		
	L DWM	1	MCA		

TABLE 2: Continued.

Patient	Location of Lesion	Lesion Size (cm^{13})	Vascular Distribution	No. of Affected Brain Regions	Time (y)
17	R SCWM	0.1	MCA	6	1
	R CB	1	SCA		
	L CGM, SCWM	60	MCA		
	L DGM	0.5	ACA		
	L CB	1	SCA		
	L CB	1	PICA		
18	R SCWM	1	MCA	3	1
	R SCWM	1	MCA		
	L SCWM	3	MCA		
	DWM*	3.5	PCA		

Note.—Each row represents one lesion. Brain regions are abbreviated as follows: R indicates right; L, left; ICA, internal carotid artery; CGM, cortical gray matter; SCWM, subcortical white matter; DWM, deep white matter; DGM, deep gray matter; CB, cerebellum; MCA, middle cerebral artery; ACA, anterior cerebral artery; PCA, posterior cerebral artery; SCA, superior cerebellar artery; AICA, anterior inferior cerebellar artery; PICA, posterior inferior cerebellar artery; BA, basilar artery. Time = days between MR imaging and angiography unless otherwise indicated.

* Lesion was in the center of the corpus callosum splenium.

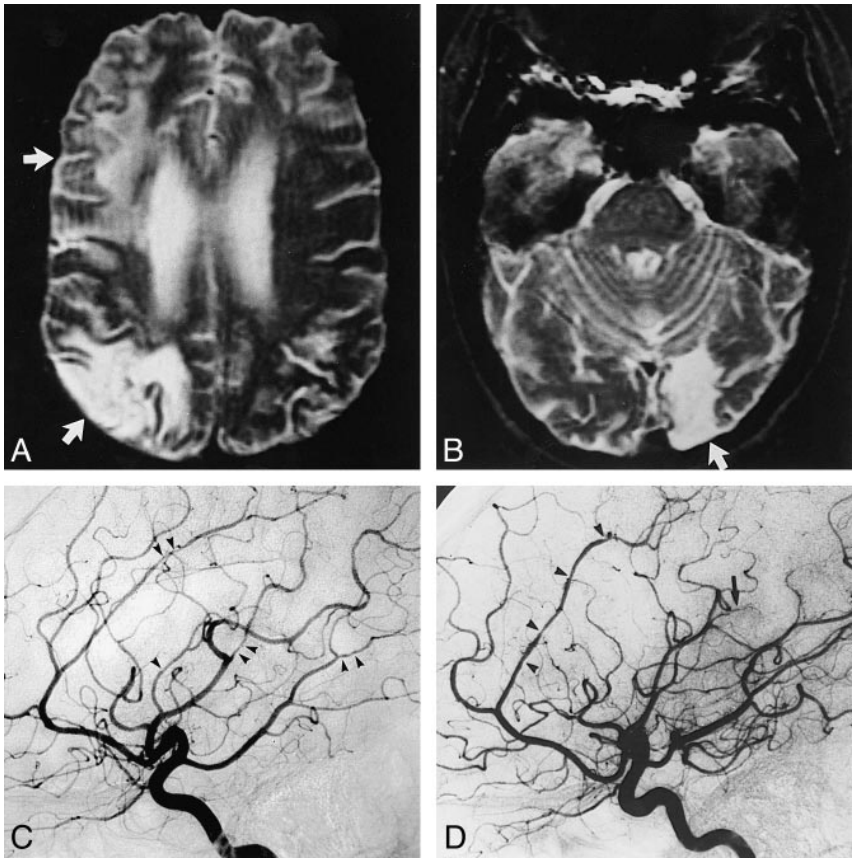

FIG 2. Patient 2: CNS vasculitis in a 37-year-old woman with systemic lupus erythematosus.

A, Axial SE MR image (3000/90) shows infarcts in the right cortical gray matter and subcortical white matter (MCA distribution, *upper arrow*; MCA/PCA watershed distribution, *lower arrow*).

B, Axial SE MR image (3000/90) shows infarcts in the left cortical gray matter and subcortical white matter (PCA distribution, *arrow*).

C, Angiogram of the left internal carotid artery shows areas of stenosis in the ACA, MCA, and PCA distributions (*arrowheads*).

D, Angiogram of the right internal carotid artery shows lesions in the ACA (pericallosal) (*arrowheads*) and severe narrowing of the distal MCA (*arrow*). Note abnormal bilateral ACAs without corresponding MR abnormality. The MR image was obtained 7 days before the angiogram.

and symptoms. In practice, however, CNS vasculitis is a rare condition. In our experience as well as that of other investigators (14), fewer than 10% of patients undergoing angiography to rule out CNS vasculitis were given that diagnosis. Enhanced understanding of the role of noninvasive testing in CNS vasculitis may facilitate these patients' evaluations. In approaching patients with possible CNS vasculitis, clinicians frequently ask neuroradiologists three questions. First, does an MR image with normal findings exclude the diagnosis of CNS vasculitis? Second, are there typical MR findings in CNS vasculitis that increase the posttest probability of CNS vasculitis and help exclude other diagnoses? Third, is the additional risk and expense of angiography justified by the information the procedure provides?

Regarding the meaning of an MR image with normal findings, our study suggests that the sensitivity of MR imaging is quite high. Indeed, among our 18 patients with CNS vasculitis, all had MR studies with abnormalities. Our findings are con-

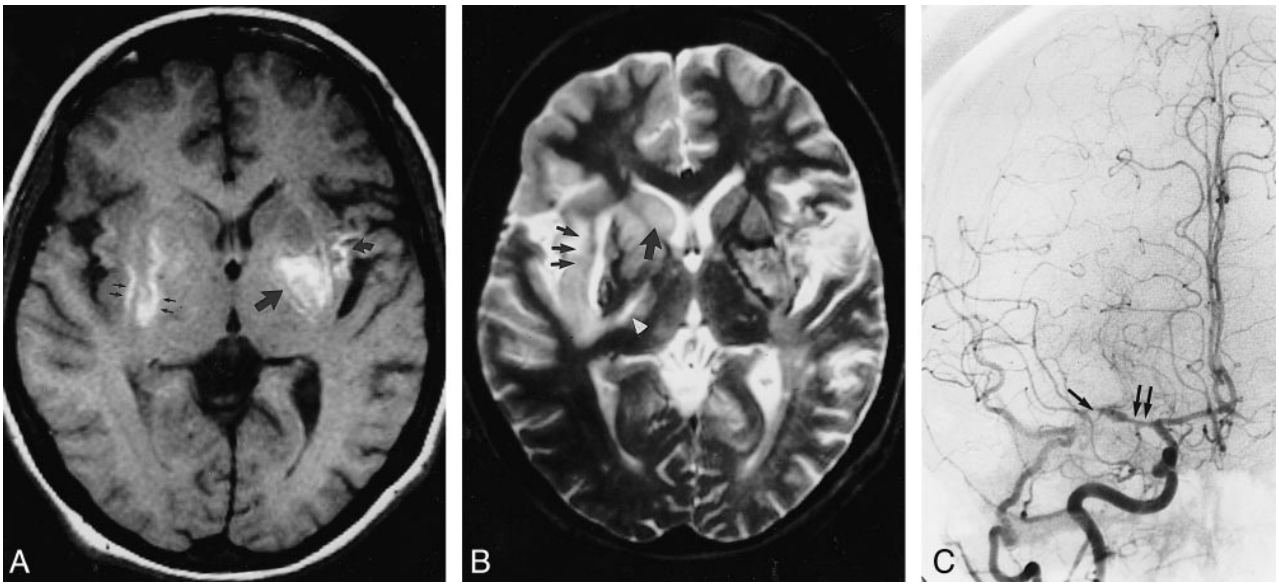

FIG 3. Patient 3: Hemorrhage in CNS vasculitis.

A, Axial SE MR image (550/25) shows T1 bright signal, consistent with hemorrhage in the left putamen (*large straight arrow*), left insular cortex (*curved arrow*), and in the region of the right external capsule (*small arrows*).

B, The corresponding T2-weighted SE image (3000/90) depicts bright signal in the basal ganglia bilaterally and particularly in the right caudate head (*large arrow*), external capsule (*small arrows*), and posterior limb, internal capsule (*arrowhead*). Abnormalities are also present in the thalami, right frontal cortex, and left periatrial white matter. The T2 bright regions are attributable to ischemia or infarction.

C, Angiogram of the right common carotid artery reveals attenuated flow in distal segments of the MCA caused by stenoses in the M1 segment (*double arrow*) and near the MCA trifurcation (*single arrow*).

sistent with the results of previous MR studies. In a review of four patients with CNS vasculitis, Vollmer et al (14) noted that MR imaging revealed substantially more lesions than CT, implying greater sensitivity. Greenan et al (15) and Harris et al (16), reporting on seven and 11 patients, respectively, with CNS vasculitis and positive angiographic findings, noted that their 18 combined patients all had abnormal MR studies. Duna and Calabrese (17) also reported a 100% sensitivity for MR imaging among seven patients with clinical diagnoses of CNS vasculitis. In contrast, Alhalabi and Moore (4), using conventional SE sequences, reported that four (24%) of 17 patients with biopsy-proved CNS vasculitis had normal MR studies. In aggregate, our results and those of others suggest that MR studies reveal abnormalities in the vast majority of patients with CNS vasculitis, and, in this sense, the sensitivity of MR imaging is quite high. However, MR imaging may not reveal all abnormal brain regions in such patients (see below).

Regarding a typical MR appearance for CNS vasculitis, the findings of our study indicate the substantial variability that may occur in CNS vasculitis. The average patient with CNS vasculitis in our study had four lesions, with a mean volume of 11.3 cm^3 per lesion; however, the range in the number of lesions per patient was wide, as was the range of infarction volumes (Figs 1 and 2). Despite this variability, the MCA distribution was affected more often than the ACA, PCA, or vertebral artery territories. Furthermore, despite the extensive collateral circulation of the subcortical white matter (18), cerebral infarctions occurred most frequently in this region. In our study, MR lesions were more evenly distributed between the gray and white matter than suggested by a previous study, which indicated a white matter predominance of lesions (4).

Although most of the lesions revealed by MR imaging were infarctions, hemorrhagic lesions also occurred. Two patients had intraparenchymal hemorrhages (patient 3, Fig 3; and patient 12) and one had SAH (patient 5, Fig 5). Thus, SAH seems to be an unusual finding in CNS vasculitis. Indeed, SAH as the sole manifestation of CNS vasculitis has been reported only once (19). In patient 6 (Fig 6), an angiogram revealed a trifurcation aneurysm of the MCA; both CT and lumbar puncture excluded SAH.

To summarize the typical appearance of CNS vasculitis on MR images, multiple subcortical infarctions are consistent with CNS vasculitis, although substantial variation in the number, size, and location of the lesions may occur in this condition. Thus, similar MR findings may occur in patients suffering from multiple sclerosis, low-grade gliomas, mitochondrial disorders, substance abuse, and other conditions (11, 14, 17, 20).

Our results indicate that in patients with CNS vasculitis, the correlation between MR imaging and angiography for individual lesions is only modest. Although each technique identified nearly the same number of lesions (66 for MR imaging and 68 for angiography; see Table 4), the correlation of specific lesions was imperfect. In our study, the majority of the MR lesions (65%) had angiographic

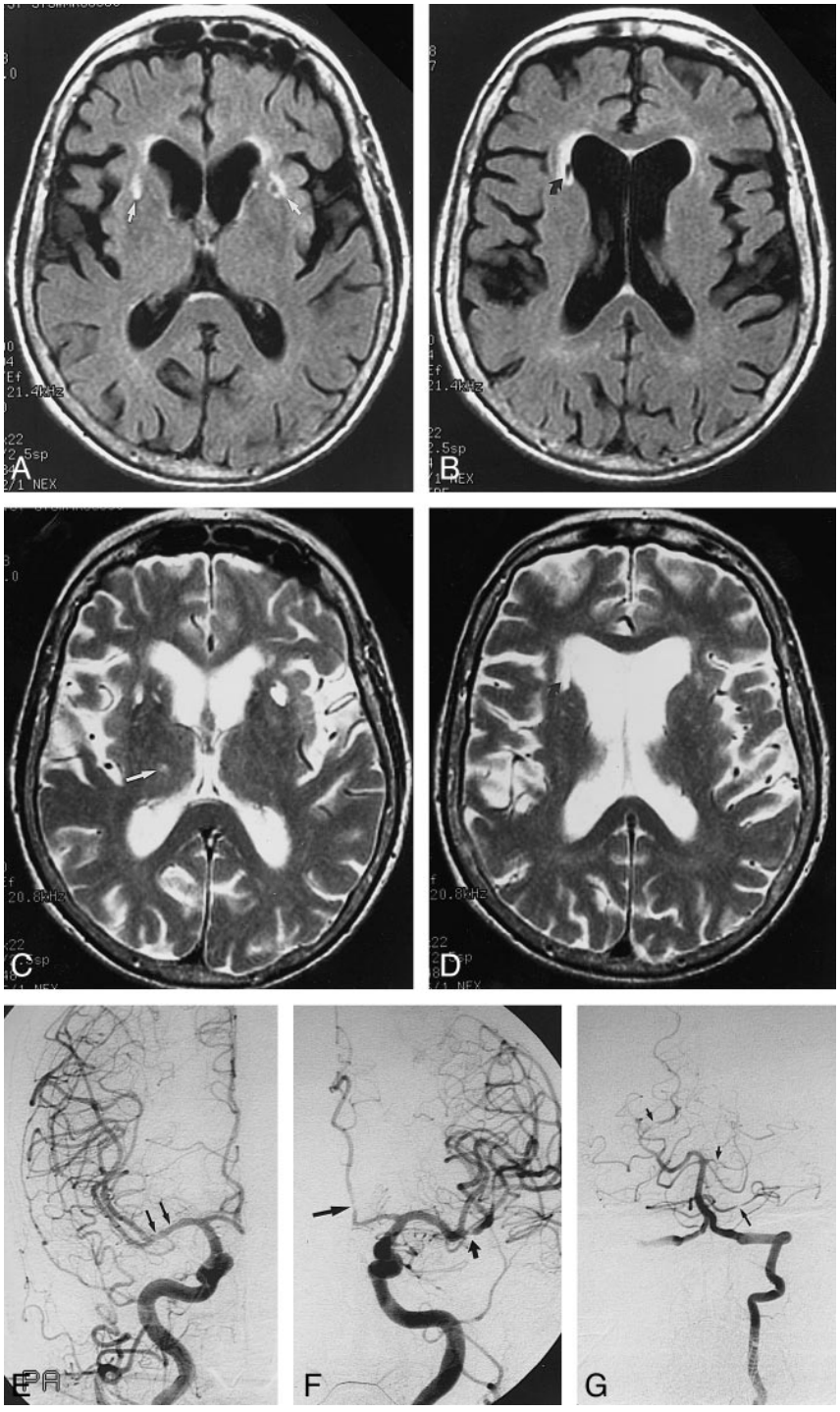

FIG 4. Patient 4: 71 year-old woman with primary angiitis of the CNS.

A and *B*, Axial FLAIR MR images (11,004/114/2200) show foci of increased signal intensity at the anterior portions of the external capsules bilaterally (*A*, *arrows*) and decreased signal adjacent to the anterior right ventricle (*B*, *curved arrow*).

C and *D*, Corresponding T2-weighted SE images (3000/91) show the lesion in the anterior right ventricle (*D, curved arrow*) and an additional lesion in the right thalamus (*C*, *arrow*).

E–G, Angiograms depict lesions in right M1 (*E, arrows*), left A2 and M2 (*F, long arrow* and *short arrow*, respectively), in both PCAs (*G, short arrows*), and in left anterior inferior cerebellar artery (*G, long arrow*).

counterparts, but some prominent MR lesions were not evident on angiograms. For example, in patient 15, the large MR infarction in the right MCA had no correlate on angiograms (Table 2). In addition, although patient 2 (Fig 2) had extensive lesions both on the MR image and the angiogram, a large right posterior cerebral infarction evident on the MR image had no corresponding lesion on the angiogram. The correlation of angiographic lesions with MR findings was worse; only a minority of angiographic lesions (44%) had correlating MR lesions (Table 4).

To our knowledge, only one other study has attempted to correlate in detail the results of MR imaging and angiography in CNS vasculitis (15). That study and ours are in agreement that only a minority (36% and 44%, respectively) of angiographic lesions correlate with MR imaging findings. Both studies also agree that the correlation of MR lesions with angiographic lesions is higher. One other

TABLE 3: Lesions detected by angiography

Patient	Diagnosis	Vessel Injected	ICA		ACA		MCA		PCA		VA		No. of Arteries Involved
			R	L	R	L	R	L	R	L	R	L	
1	PACNS	R ICA L CCA, L VA	−	−	A3	A1	M2	M1	P1, P3	Occl	SCA	PICA	8
2	SLE	R CCA, L CCA, L VA	−	−	+	−	+	+	−	+	−	−	4
3	PACNS	AA, R ICA, L ICA, L VA, R VA	−	Occl	−	−	M1, M2	−	−	−	+	−	3
4	PACNS	R CCA, L CCA, L VA	−	−	−	A2	M1	M2	+	+	−	AICA	6
5	PACNS	R CCA, L CCA, L VA	−	−	+	+	+	+	−	−	−	−	4
6	PACNA	R ICA, L CCA, L VA	−	−	+	−	−	M1, M2	−	+	−	−	3
7	PACNS	R CCA, L CCA, L VA	−	−	−	A2, A3	M3	M2	−	−	−	−	3
8	PACNS	R ICA, L ICA, L VA	−	−	A3	A3	M3	M3	+	+	−	−	6
9	PACNS	R CCA, R VA	−	NE	−	NE	M2	NE	−	−	−	−	1
10	PACNS	R CCA, L CCA, L VA	+	−	+	+	−	M3	+	+	−	PICA	8
11	PACNS	R CCA, L CCA, L VA	+	+	A1	−	M1	M1	P1, P2	P1, P2	−	−	7
12	PACNS	R CCA, L CCA, L VA	−	−	A3	−	−	−	−	P2	−	−	2
13	PACNS	R CCA, L CCA L VA	−	−	+	+	+	+	Occl	Occl	−	−	6
14	PACNS	R CCA, L CCA	+	+	A1	A3	−	M1	−	−	NE	NE	5
15	PACNS	R CCA, L ICA, L VA	−	−	A1	A1	M1	M1	−	−	−	−	4
16	SLE	R ICA, L ICA, L VA	−	−	−	+	−	−	−	−	−	−	1
17	PAN	AA, R ICA, L ICA, L VA	−	−	−	−	−	M2	−	−	−	−	1
18	GCA	AA, R CCA, L CCA	+	+	−	−	−	−	−	−	−	−	2

Note.—L indicates left; R, right; AA, aortic arch; CCA, common carotid artery; ICA, internal carotid artery; VA, vertebral artery; ACA, anterior cerebral artery; MCA, middle cerebral artery; PCA, posterior cerebral artery; SCA, superior cerebellar artery; PICA, posterior inferior cerebellar artery; AICA, anterior inferior cerebellar artery; PACNS, primary angiitis of the CNS; SLE, systemic lupus erythematosus; PAN, polyarteritis nodosa; GCA, giant cell arteritis; Occl, occluded; NE, not evaluated. Where possible, segments were assigned to appropriate segments of the corresponding vascular distribution. "+" indicates an artery affected with multiple lesions (*eg*, beading); "−" indicates an unaffected artery.

TABLE 4: MR imaging versus angiography: correlation of lesions

MR imaging		
Total MR lesions: 66	No. of MR lesions evident on angiogram: 43	Percentage of MR lesions evident on angiogram: 65%
Angiography		
Total abnormal vessels: 68	No. of angiogram lesions evident on MR: 30	Percentage of angiogram lesions evident on MR: 44%

study, which did not attempt a detailed correlation of the two imaging techniques, simply concluded that brain abnormalities identified at MR imaging were less extensive than those delineated angiographically (4).

The discrepancies between MR imaging and angiography may have several explanations. First, the differences may be attributed to the different times at which the studies were performed. This seems unlikely, since the great majority of studies were performed in close succession. Second, a patient with vascular narrowing but no tissue infarction might have an angiogram with positive results but an MR image with negative results (conversely, small-vessel abnormalities not apparent on an angiogram might lead to infarction detectable by MR imaging). Finally, subtle MR abnormalities may escape detection unless special sequences or orientations are obtained (Fig 5).

Our results emphasize that angiography often provides additional information about the extent of disease beyond that detected by MR imaging. For

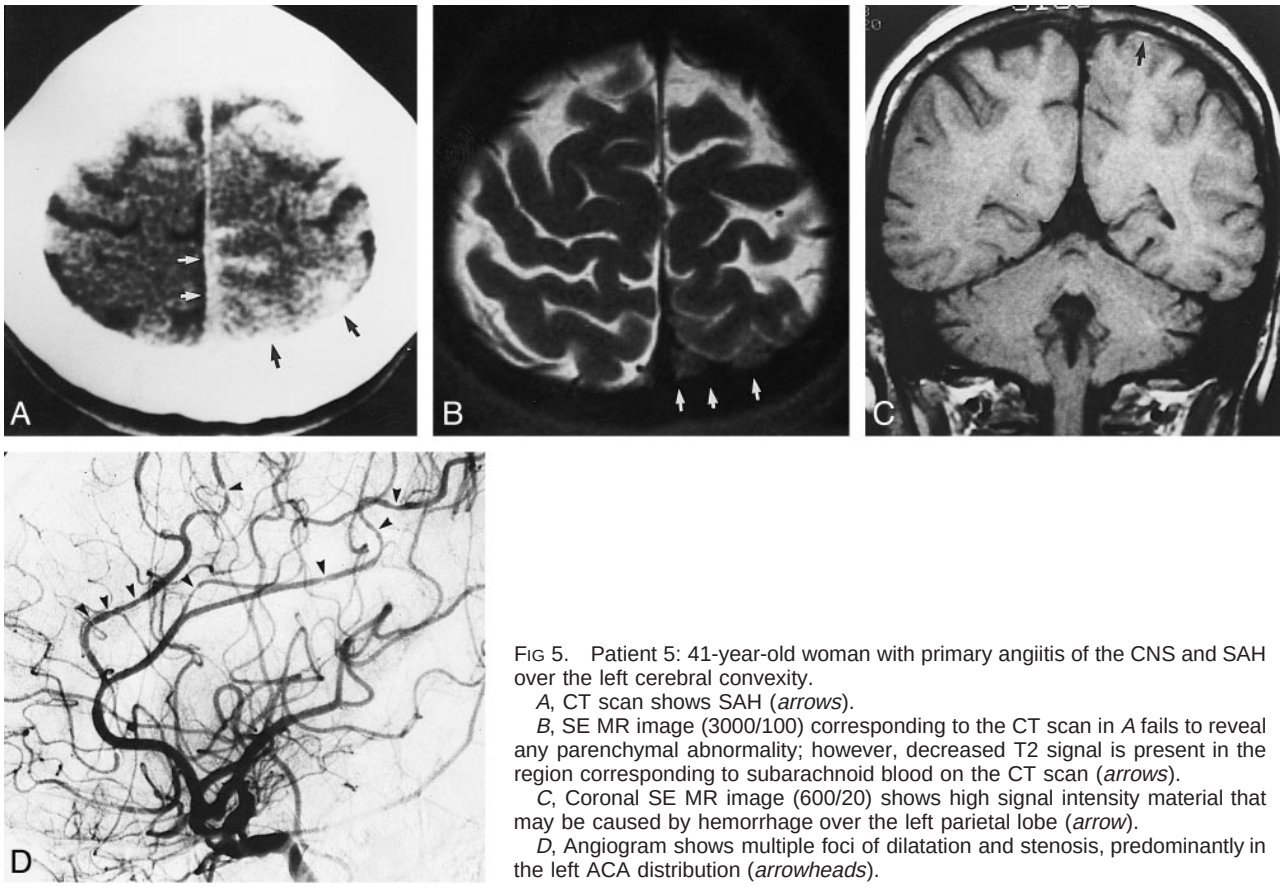

FIG 5. Patient 5: 41-year-old woman with primary angiitis of the CNS and SAH over the left cerebral convexity.

A, CT scan shows SAH (*arrows*).

B, SE MR image (3000/100) corresponding to the CT scan in *A* fails to reveal any parenchymal abnormality; however, decreased T2 signal is present in the region corresponding to subarachnoid blood on the CT scan (*arrows*).

C, Coronal SE MR image (600/20) shows high signal intensity material that may be caused by hemorrhage over the left parietal lobe (*arrow*).

D, Angiogram shows multiple foci of dilatation and stenosis, predominantly in the left ACA distribution (*arrowheads*).

example, the angiographic findings may offer an explanation for a patient's signs and symptoms that cannot be attributed to the abnormalities seen on MR images. Moreover, findings of serial studies of patients with CNS vasculitis have shown that response to treatment is more likely to be evident on angiograms than on MR images (4).

Our study has several limitations. First, CNS vasculitis is a difficult entity to define, because the diagnosis can rarely be established by a single test (2, 8, 9, 11). All imaging techniques, including MR imaging and angiography, have imperfect specificity; even brain biopsies yield high false-negative rates (4, 11, 15). In the absence of pathologic confirmation, the diagnosis of CNS vasculitis needs to be based on careful evaluation of clinical signs and symptoms, correlation with radiologic findings, and exclusion of other causes (8, 16, 21). Because this approach is not infallible, some of our patients may have been misdiagnosed. Our thorough clinical and radiologic review of these patients reduces that possibility but can never eliminate it entirely.

Because many of our patients were studied between 1986 and 1990, only six had MR angiographic studies. Despite the value of MR angiography in patients with medium- and large-vessel disease (22), the resolution of MR angiography remains insufficient for the fine vascular abnormalities that frequently accompany CNS vasculitis (22–24).

Use of a FLAIR sequence in conjunction with our routine SE sequences would probably have increased the sensitivity of MR imaging (25, 26). FLAIR imaging is particularly sensitive for periventricular and superficial cortical infarctions (27); however, FLAIR may be inferior to conventional long-TR imaging in detecting posterior fossa lesions (28, 29). Furthermore, criteria for normal FLAIR images are still being formulated (30). Because the technique has been available only routinely at our institution since 1995, only one patient underwent FLAIR imaging. In that patient (patient 4, Fig 4), the deep gray matter lesions were equally evident on the T2-weighted and FLAIR sequences, and one right-sided thalamic lesion would have been missed had FLAIR imaging been used alone. Although FLAIR imaging should be performed in all patients with possible CNS vasculitis, it should be used in conjunction with, rather than in lieu of, conventional SE sequences.

Finally, failure to use contrast medium in all the MR studies was another potential limitation. Administration of contrast material increases the detection of small infarctions on MR images (31) and may also be useful in estimating the age of a lesion. However, because of the retrospective nature of the study design, this limitation could not be remedied.

Other imaging techniques with the potential to enhance lesion detection and define brain regions

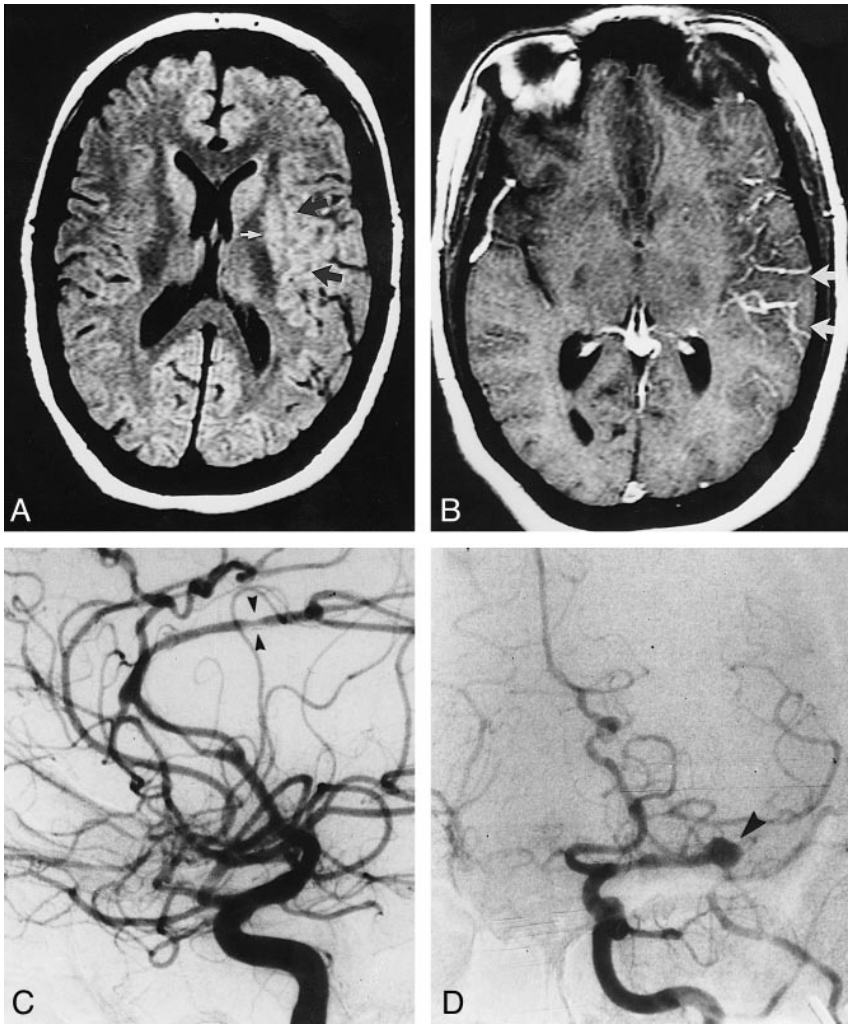

FIG 6. Patient 6: 24-year-old woman with primary angiitis of the CNS.

A, Axial SE MR image (1500/30) shows high signal intensity in the left parietal cortex, subcortical white matter (*black arrows*), and in the left putamen (*white arrow*).

B, Contrast-enhanced axial SE MR image (550/25) shows vascular and mild parenchymal enhancement (*arrows*). The vascular stasis is indicative of acute cerebral ischemia.

C, Right internal carotid artery angiogram shows narrowing in the right pericallosal artery (*arrowheads*). Superimposition of vessels immediately distal to that lesion gives the appearance of an aneurysm.

D, Left common carotid artery angiogram reveals attenuated MCA branches distal to a trifurcation aneurysm (*arrowhead*).

at risk in CNS vasculitis include perfusion- and diffusion-weighted imaging, MR spectroscopy, and positron emission tomography. These techniques may become increasingly important as more effective therapies for CNS vasculitis become available. Perfusion- and diffusion-weighted imaging may be superior to FLAIR imaging in the detection and characterization of early lesions (32).

Conclusion

MR imaging is very sensitive for CNS vasculitis and typically shows supratentorial infarctions in the cortical and subcortical regions; however, the MR appearance is not specific for CNS vasculitis. Furthermore, the correlation between MR imaging and angiography on specific lesions is only moderate. Our results suggest that these two imaging techniques provide different information about the extent of CNS vasculitis. For a complete assessment of the vascular damage resulting from CNS vasculitis, both imaging techniques should be used.

Acknowledgments

We thank Edward Herskovits for serving as arbitrator for the MR and angiographic studies and Tammy Noethen for word processing the manuscript.

References

1. Ferris EJ, Levine HL. **Cerebral arteritis: classification.** *Radiology* 1973;109:327–341
2. Calabrese LH, Fulan AJ, Gragg LA, Trumane J. **Primary angiitis of the central nervous system: diagnostic criteria and clinical approach.** *Cleve Clin J Med* 1992;59:293–306
3. Cupps TR, Moore PM, Fauci AS. **Isolated angiitis of the central nervous system: prospective diagnostic and therapeutic experience.** *Am J Med* 1983;74:97–105
4. Alhalabi M, Moore PM. **Serial angiography in isolated angiitis of the central nervous system.** *Neurology* 1994;44:1221–1226
5. Mitsias P, Levine SR. **Large cerebral vessel occlusive disease in systemic lupus erythematosus.** *Neurology* 1994;44:385–393
6. Kissel JT. **Neurologic manifestations of vasculitis.** *Neurol Clin* 1989;7:655–673
7. Wynne PJ, Younger DS, Khandji A, Silver AJ. **Radiographic features of central nervous system vasculitis.** *Neurol Clin* 1997;15:779–804
8. Moore PM. **Vasculitis of the central nervous system.** *Semin Neurol* 1994;14:307–312
9. Calabrese LH, Mallek JA. **Primary angiitis of the central nervous system: report of 8 new cases, review of the literature, and proposal for diagnostic criteria.** *Medicine* 1987;67:20–39

10. Stone JH, Pomper MG, Roubenoff R, Miller TJ, Hellmann DB. **Sensitivities of noninvasive tests for central nervous system vasculitis: a comparison of lumbar puncture, computed tomography and magnetic resonance imaging.** *J Rheumatol* 1994; 21:1277–1282
11. Duna GF, Calabrese LH. **Limitations of invasive modalities in the diagnosis of primary angiitis of the central nervous system.** *J Rheumatol* 1995;22:662–667
12. Hellmann DB, Roubenoff R, Healy R, Wang H. **Central nervous system angiography: safety and predictors of a positive result in 125 consecutive patients evaluated for possible vasculitis.** *J Rheumatol* 1992;19:568–572
13. Kretschmann HG, Weinrich W. **Cranial Neuroimaging and Clinical Neuroanatomy.** New York: Thieme; 1992
14. Vollmer TL, Guamaccia J, Harrington W, Pacia SV, Petroff OAC. **Idiopathic granulomatous angiitis of the central nervous system: diagnostic challenges.** *Arch Neurol* 1993;50:925–930
15. Greenan TJ, Grossman RI, Goldberg HI. **Cerebral vasculitis: MR imaging and angiographic correlation.** *Radiology* 1992;182:65–72
16. Harris KG, Tran DD, Sickels WJ, Cornell SH, Yuh WTC. **Diagnosing intracranial vasculitis: the roles of MR and angiography.** *AJNR Am J Neuroradiol* 1994;15:317–330
17. Duna GF, Calabrese LH. **Limitations of invasive modalities in the diagnosis of primary angiitis of the central nervous system.** *J Rheumatol* 1995;22:662–667
18. Osborn AG. **Diagnostic Neuroradiology.** St Louis: Mosby; 1994; 330–398
19. Biller J, Loftus CM, Moore SA, et al. **Isolated central nervous system angiitis first presenting as spontaneous intracranial hemorrhage.** *Neurosurgery* 1987;20:310–315
20. Calabrese LH. **Vasculitis of the central nervous system.** *Rheum Dis Clin North Am* 1995;21:1059–1076
21. Miller DH, Ormerod IEC, Gibson A, de Boulay EDGH, Rudge P, McDonald WI. **MR brain scanning in patients with vasculitis: differentiation from multiple sclerosis.** *Neuroradiology* 1987;29: 226–231
22. Dagirmanjian A, Ross JS, Obuchowski N, et al. **High resolution, magnetization transfer saturation, variable flip angle, time-of-flight MRA in the detection of intracranial vascular stenoses.** *J Comput Assist Tomogr* 1995;19:700–706
23. Stellar RJ. **Imaging blood vessels of the head and neck.** *J Neurol Neurosurg Psychiatry* 1995;59:225–237
24. Stock KW, Radue EW, Jacob AL, Bao XS, Steinbrich W. **Intracranial arteries: prospective blinded comparative study of MR angiography and DSA in 50 patients.** *Radiology* 1995;195:451–456
25. Kates R, Atkinson D, Brant-Zawadski M. **Fluid-attenuated inversion recovery (FLAIR): clinical prospectus of current and future applications.** *Top Magn Reson Imaging* 1996;8:389–396
26. Tourbah A, Deschamps R, Stievenart JL, et al. **Magnetic resonance imaging using FLAIR pulse sequence in white matter diseases.** *J Neuroradiol* 1996;23:217–222
27. Thurnher MM, Thurnher SA, Fleischmann D, et al. **Comparison of T2-weighted and fluid-attenuated inversion-recovery fast spin-echo MR sequences in intracerebral AIDS-associated disease.** *AJNR Am J Neuroradiol* 1997;18:1601–1609
28. Gawne-Cain ML, O'Riordan JI, Coles A, Newell B, Thompson AJ, Miller DH. **MRI lesion volume measurement in multiple sclerosis and its correlation with disability: a comparison of fast fluid attenuated inversion recovery (fFLAIR) and spin echo sequences.** *J Neurol Neurosurg Psychiatry* 1998;64:197–203
29. Gawne-Cain ML, O'Riordan JI, Thompson AJ, Moseley IF, Miller DH. **Multiple sclerosis lesion detection in the brain: a comparison of fast fluid-attenuated inversion recovery and conventional T2-weighted dual spin echo.** *Neurology* 1997;49:364–370
30. Gawne-Cain ML, Silver NC, Moseley IF, Miller DH. **Fast FLAIR of the brain: the range of appearances in normal subjects and its application to quantification of white-matter disease.** *Neuroradiology* 1997;39:243–249
31. Miyashita K, Naritomi H, Sawada T, et al. **Identification of recent lacunar lesions in cases of multiple small infarctions by magnetic resonance imaging.** *Stroke* 1988;19:834–839
32. Flacke S, Keller E, Hartmann A, et al. **Improved diagnosis of early cerebral infarct by the combined use of diffusion and perfusion imaging.** *Rofo Fortschr Geb Rontgenstr Neuen Bildgeb Verfahr* 1998;168:493–501